THE UNIVERSITY OF NEW SOUTH WALES
SCHOOL OF CIVIL AND ENVIRONMENTAL ENGINEERING
WATER RESEARCH LABORATORY

A LABORATORY STUDY OF WAVE GROWTH AND AIR FLOW BEHAVIOUR OVER WAVES STRONGLY FORCED BY WIND

WRL Research Report 219 01/07/04

by

W L Peirson and S E Pells

Report Documentation Page

Form Approved
OMB No. 0704-0188

1. REPORT DATE	2. REPORT TYPE	3. DATES COVERED
01 JUL 2004	**N/A**	**-**

4. TITLE AND SUBTITLE	5a. CONTRACT NUMBER
A Laboratory Study Of Wave Growth And Air Flow Behaviour Over Waves Strongly Forced By Wind	5b. GRANT NUMBER
	5c. PROGRAM ELEMENT NUMBER
6. AUTHOR(S)	5d. PROJECT NUMBER
	5e. TASK NUMBER
	5f. WORK UNIT NUMBER
7. PERFORMING ORGANIZATION NAME(S) AND ADDRESS(ES) **Water Research Laboratory School of Civil and Environmental Engineering University of New South Wales King Street Manly Vale NSW 2093 Sydney, Australia**	8. PERFORMING ORGANIZATION REPORT NUMBER
9. SPONSORING/MONITORING AGENCY NAME(S) AND ADDRESS(ES)	10. SPONSOR/MONITOR'S ACRONYM(S)
	11. SPONSOR/MONITOR'S REPORT NUMBER(S)

12. DISTRIBUTION/AVAILABILITY STATEMENT
Approved for public release, distribution unlimited

13. SUPPLEMENTARY NOTES
The original document contains color images.

14. ABSTRACT

15. SUBJECT TERMS

16. SECURITY CLASSIFICATION OF:			17. LIMITATION OF ABSTRACT	18. NUMBER OF PAGES	19a. NAME OF RESPONSIBLE PERSON
a. REPORT	b. ABSTRACT	c. THIS PAGE			
unclassified	**unclassified**	**unclassified**	**UU**	**29**	

Water Research Laboratory
School of Civil and Environmental Engineering
University of New South Wales ABN 57 195 873 179
King Street
Manly Vale NSW 2093 Australia

Telephone: +61 (2) 9949 4488
Facsimile: +61 (2) 9949 4188

Research Report No 219
Report Status Draft Final
Date of Issue July 2004

ISBN TBA

The work reported herein was carried out at the Water Research Laboratory, School of Civil and Environmental Engineering, University of New South Wales in Sydney, Australia.

This study was undertaken on behalf of the United States Army, European Reseach Office Funding under contract number N62558-04-M-0002.
Approved for public release; distribution is unlimited.

CONTENTS

LIST OF FIGURES

1. INTRODUCTION

Existing normalisations of wave response to prevailing winds remain unreconciled with theoretical predictions. Accurate predictive schemes are essential for the intense storms that are responsible for the most severe wave fields but show signficant complexity as observed by Wright *et al.* (2001).

Using the experimental techniques used successfully to study the attenuation of waves by opposing winds (Peirson, Garcia and Pells, 2003 and hereafter PGP03), a study was proposed for the growth phase to examine a normalisation proposed by Peirson and Belcher (2003) which appears to reconcile observed scatter in wind-wave growth observations.

In addition, it is proposed to observe wave growth and air flow behaviour for steep wave fields near and at the transition to the breaking condition. The new normalisation predicts close coupling of the momentum and energy fluxes with existing observations for this condition restricted to a very small and limited data set.

Until recently, theoretical parameterisations of wave growth due to wind have been based on the inviscid theory of Miles (1957) which predicts energy input levels that are substantially too low. To provide wind energy input levels that are consistent with laboratory and field measurements, the coefficients in Miles theory have been substantially increased in spite of no sound theoretical justification. Measured values of wave growth show scatter around the modified parameterisation of between a factor of 2 and 4.

Recent studies by PGP03 developed a much simpler normalisation of wind-wave interaction for the attenuation phase (the case when wind is opposed to existing wave systems). The findings of this investigation has an explanation for the behaviour of wave fields observed by Wright *et al.* (2000) within hurricanes which was previously not possible in view of the low rates of wave attenuation estimated by previous investigators.

As shown by Peirson and Belcher (2003), normalisation of existing wave growth data with that developed for wave attenuation is able to reconcile data from a much wider range of sources with scatter consistent with estimated errors in the measurements. Peirson and Belcher also show that the energy flux rate from wind to waves has a strong relationship with the momentum flux consistent with the sheltering theory of Jeffreys (1924, 1925).

A study of Banner (1990) has shown that strong transitions in the momentum flux occur with the onset of wave breaking. It appears that the energy flux will remain strongly related to the momentum

flux but this is yet to be tested. This transition occurs at the high wave steepnesses found within intense cyclonic storms. The transition to breaking also marks the onset of air flow separation above the waves.

In spite of these important observations, few investigators have reported mean wave steepness which is a critical parameter in this new normalisation. There is a pressing need for suitable data to test the developed normalisation.

This report describes laboratory measurements of wave growth rates under coflowing wind conditions with measurement of total momentum flux accompanied by preliminary observations of air flow behaviour over the freely propagating waves.

2. METHOD

2.1 Theory

The diversity and duplication of notation within the wind-wave interaction discipline is a source of continuing confusion. In this paper, we follow the notation of Komen *et al.*, 1994 (especially Section I.2.5, p.25*ff*).

The local total energy density of surface waves propagating past a point can be evaluated as:

$$E = F = \rho_w g \langle \eta^2 \rangle = \rho_w g \int \int F(f, \theta) df \, d\theta \tag{1}$$

where E is the total local energy density, ρ_w is the density of water, g is gravitational acceleration, η is the instantaneous water surface elevation, the angle brackets indicate time-averaging, F is the spectral energy density as a function of wave direction θ and wave frequency f.

In this investigation we are concerned with the development of mechanically-generated wave energy along the axis of a laboratory tank. Directional components will not and need not be considered.

The wave energy balance equation is (for example, Komen *et al*., 1994, pages 33 and 47):

$$\frac{dF(\omega, \theta)}{dt} = S_{in}(\omega, \theta) + S_{nl}(\omega, \theta) + S_{diss}(\omega, \theta) + S_{bed}(\omega, \theta) \tag{2}$$

where S_{in} is the energy input from the wind, S_{nl} are non-linear energy transfers due to wave-wave interactions and S_{diss} (a negative quantity) is the loss of energy from the wave field. Note that the above equation uses the total derivative and therefore considers changes moving with the group velocity of the waves.

When the wind is in the same direction and has a higher speed than the propagating waves, the ensuing drag on the waves which results in an energy flux to the wave field, S_{in}.

S_{nl} describes the transfers of energy between different wave frequencies within a wave spectrum. Two types of non-linear interactions have been identified in the literature:

1. Within wind-forced wave fields, non-linear transfers can occur via interacting directional spectral components. Here, we are considering the behaviour of monochromatic, monodirectional waves that have a relatively low frequency in comparison with any wind-generated waves. Whilst the effects of nonlinear interactions between the wind-generated microscale waves may be important, nonlinear interactions do not exist for the low frequency monochromatic waves.

2. Benjamin and Feir (1967) showed that monochromatic wave trains are theoretically unstable with energy flux from the fundamental due to sideband instabilities. Bliven *et al.*(1986) have shown that sideband instabilities do not develop in the presence of wind.

Changes in surface wave energy due to dissipative processes (S_{diss}) are generally attributed to wave breaking or interactions between the waves and fluid boundaries. The experiments described here were designed to avoid breaking at the scale of the mechanically-generated waves. Theories for the loss of wave energy due to boundary interaction via viscosity have received experimental verification by the studies of Mitsuyasu and Honda (1982, hereafter MH82) and their results are used in this investigation. However, as discussed in PGP03, because a wider tank has been used than that of MH82, the viscous attenuation rates were found to be too small to measure. Following the approach of MH82, the small wave attenuation rates due to viscous effects have been added to the measured growth rates during this study so that the total growth directly attributable to wind-induced effects can be obtained.

For low-frequency, monochromatic, monodirectional waves of frequency f_p in the absence of wave breaking and non-linear interactions, equation 2 becomes:

$$\frac{\partial F}{\partial t} = S'_{\text{in}} \tag{3}$$

Where the observed wave growth rate S'_{in} is less than the actual wind input S_{in} due to the effects of S_{visc} the viscous attenuation due to interaction between waves and the surface and the side walls:

$$S'_{\text{in}} = S_{\text{in}} + S_{\text{visc}} \tag{4}$$

2.2 Measurement Techniques

The development of wave energy due to wind action has been measured using the techniques proposed by Bole (1967) and MH82. Ensemble measurements of surface variance (equation 1) are taken at a sequence of locations along a wave tank as shown in Figure 1. From these measurements changes in wave energy distance can be obtained.

If a wave packet exposed to a steady wind does not change its group speed rapidly with time, we can evaluate the local time-dependent wave growth rate as:

$$\frac{dF}{dt} = \frac{\partial F}{\partial t} + c_g \frac{\partial F}{\partial x} = c_g \frac{\partial F}{\partial x} \tag{5}$$

where c_g is the group wave speed (the speed at which wave energy propagates) and x is distance in the direction of the low-frequency wave propagation. For deepwater waves, $c_g = c/2$ where c is the wave phase speed. In these experiments, we have used a steady wind and the term $\partial F/\partial t = 0$.

Wave growth rates are usually expressed in a time-based dimensional form as $\gamma = 1/F\, dF/dt$ or as the non-dimensional quantity γ/f .

A difficulty with this technique is that as well as developing low-frequency waves, the wind also generates a spectrum of the high-frequency microscale waves (0.05m<λ<0.4m). MH82 extracted the growth rate of the low frequency waves (f_p<1.3Hz, λ>0.8m) using spectral filtering techniques to obtain the wave energy contained in the frequency band $0.9f_p \rightarrow 1.1f_p$.

2.3 Wind-Wave Facility

These experiments were undertaken in the main wind-wave tank at the Water Research Laboratory. Overall tank dimensions are length 30 m, width 0.9 m and height 1.55m. The layout of this tank is shown in Figure 1.

Waves are generated by a controlled random generator at one end of the tank. During these investigations, only monochromatic waves were investigated. At the far end, a dissipating beach was installed.

The tank is roofed with flow in the air cavity controlled by a large fan fitted at the opposite end to the wave generator. For these investigations, water depth in the tank was 1.10m giving a mean air cavity depth of 0.45 m. Wind speeds in the air cavity were monitored using a hot bulb anemometer mounted from the roof at mid-height within the air cavity at the location shown. The roof was profiled to create zero pressure gradient along the tank at the midpoint of the test section. This was undertaken to provide suitable conditions for profile measurements of total stress as described in Section 2.4.

Previous testing had shown that the reflected waves generated by the incidence of small paddle waves were reduced to less than 2% of the incident wave amplitude. Reflected waves were indistinguishable amongst the (small, <2%) crosstank oscillations that were also generated and therefore did not contribute any significant systematic error (PGP03, p. 351).

Wind forcing of the surface was monitored using a hot bulb anemometer measuring wind speed located approximately 2m downwind of the air inlet (Figure 1).

2.4 Wind Measurements

Local measurements of the wind stress were obtained by measuring the near-surface logarithmic boundary layer profiles in the air for each wind speed condition. These were taken at the midpoint of surface variance measurement along the tank.

The velocity measurements were obtained from a small pitot tube with its pressure ports connected to a Barocel micromanometer. Output from the Barocel was connected to a data acquisition computer sampling at 100Hz.

Local measurements of the wind stress were taken for several wind/wave conditions as the results of Bliven *et al.* (1986) and Banner (1990) show a systematic increase in observed total stress with increasing mean wave steepness.

2.5 Wave Measurements

During this investigation, water surface elevation was monitored using capacitance wave gauges fitted with fine (~200 μm diameter) wire filaments. Each gauge had a range of approximately 200 mm. These were carefully and regularly calibrated and over the period of testing showed a gain repeatibility better than 2%. Eight probes were used, located at distances of 1.5, 2.5, 4.0, 6.0, 7.5, 9.0 and 10.0 m from the first probe within the roofed section (see Figure 1).

The water surface elevation measurements of the wave probes were recorded at a frequency of 40 Hz per channel by a computer with an analogue to digital converter. These data were stored for subsequent processing.

2.6 Data Processing

Fast Fourier Transforms (FFTs) were used to process 2048 data points from each record (approximately 50s) to determine the local wave energy.

A well-established observation (Mitsuyasu, 1966) is that wind waves are attenuated by underlying swell. In all of our experiment conditions, microscale wave activity declined as the steepness of low-frequency mechanically-generated waves increased.

Energy associated with the low frequency waves was identified within the complete spectrum by integrating the energy within a frequency band between $0.9 f_p \rightarrow 1.1 f_p$. The frequency band was

selected to be as narrow as possible to ensure that energy associated with low frequency waves was captured whilst the high-frequency wind wave energy was not included.

To quantify γ from point measurements of wave energy along the tank, a model of wave attenuation must be fitted to the data. Consistent with previous investigators, we assume exponential growth:

$$E = E_0 e^{\Delta x} \tag{6}$$

In each case, Δ was determined from the measured data by a least-squares fit of this equation to the measured energy as a function of fetch. Non-dimensional attenuation rates were determined from:

$$\frac{\gamma}{f} = \frac{\dot{E}}{fE} = \frac{c_g}{fE}\frac{\partial E}{\partial x} = \frac{(\Delta + \Delta_{visc})c}{2f} \tag{7}$$

where Δ_{visc} is the estimated attenuation rate due to viscosity at the surface and the walls of the tank based on the work of Van Dorn, 1966.

Similar to the approach adopted in PGP03, the The process of least-squares fitting yields a correlation coefficient *r* which can be related to a confidence interval for Δ of:

$$\frac{\pm t^p \sqrt{(1-r^2)}}{\sqrt{(n-2)}} \frac{\sigma(\ln(E/E_0))}{\sigma(x)}$$

where t^p is the value from the *Student's t distribution* for confidence limits of *p*%, σ signifies the standard deviation and *x* are the positions of *n* wave probes. (See Acton, 1959, p. 24) For this investigation we selected *p*=90%.

3. RESULTS

3.1Wind Stress Measurements

Wind stress measurements comparable with this study were obtained by MH82 (summarised in Table 1) and our previous study (PGP03, Table 2). The measurements of this study are presented in Table 3.

For all these studies, the stress measurements were obtained by measuring the logarithmic profile immediately above the wave crests and deriving values of u_*^a and z_0 from fits to the measured data. If one accepts errors in the measured values of 20 and 50% respectively, the values measured by MH82 and PGP03 are consistent.

Table 1. Friction velocities and roughness lengths obtained by MH82 from wind profile measurements over a water surface not contaminated by surfactant.

U_{cl} (ms^{-1})	u_*^a (ms^{-1})	z_0 (mm)
5.0	0.224	0.036
7.5	0.324	0.035
10.0	0.478	0.129
12.5	0.625	0.221
15.0	1.103	1.083

Table 2. Friction velocities and roughness lengths obtained by PGP03 from wind profile measurements in the absence of mechanically-generated waves.

U_{cl} (ms^{-1})	u_*^a (ms^{-1})	z_0 (mm)
5	0.192	0.0068
7	0.315	0.034
9	0.422	0.049
11	0.579	0.147
15	1.050	0.846

Table 3. Friction velocities and roughness lengths obtained from wind profile measurements during this investigation

U_{cl} (ms^{-1})	f_p (Hz)	ak_p	u_*^a (ms^{-1})	z_0 (mm)
4.80		0.000	0.310	0.37
4.80	0.77	0.063	0.296	0.15
4.80	0.77	0.188	0.489	2.03
4.80	1.11	0.094	0.348	0.60
4.80	1.11	0.188	0.711	9.34
4.80	1.43	0.094	0.310	0.56
4.80	1.43	0.188	0.335	0.48
7.20		0.000	0.472	0.63
7.20	0.77	0.063	0.449	0.29
7.20	0.77	0.188	0.579	0.98
7.20	1.11	0.094	0.522	0.97
7.20	1.11	0.188	0.891	6.13
7.20	1.43	0.094	0.442	0.56
7.20	1.43	0.188	0.475	0.64
9.25		0.000	0.572	0.82
9.25	0.77	0.063	0.533	0.30
9.25	0.77	0.188	0.855	2.58
9.25	1.11	0.094	0.736	1.98
9.25	1.11	0.188	1.247	9.83
9.25	1.43	0.094	0.714	1.99
9.25	1.43	0.188	0.881	3.50

By comparison, the fitted values of u_*^a and z_0 obtained from the velocity profiles during this study are considerably (~50%) higher. The wind stress profiles are summarised in Figures 2 to 4. Even casual inspection shows that the current profiles are exhibiting significantly different stress behaviour from those obtained during the attenuation study.

As discussed earlier, the only change in physical arrangement of the tank from that of the attenuation study was that the roof was profiled along the test section. This change was made because of concerns expressed by Prof. Mark Donelan at the Waves and Operational Oceanography Workshop in Brest, France in June 2003 regarding pressure gradients along the tank.

However, the seminal study of Kline *et al.*(1966) only indicates negligible changes in the estimates of u_*^a obtained from logarithmic profiles for boundary layers with no pressure gradient and those with the non-dimensional pressure gradients imposed by the air cavity geometry during the attenuation study. In addition, Kawamura (1981) has shown that use of the logarithmic method is reliable for obtaining the wind stress over wind-forced wave fields. At this stage, we have not been able to resolve this issue.

Similar to the findings of Bliven *et al.* (1986), our measurements show a significant and systematic increase in u_*^a with increasing steepness of the mechanically-generated waves. To our knowledge, this is the first study that has presented this enhancement in the stress across a range of peak spectra periods. Given the current uncertainties in the values of friction velocity appropriate to these experiments, we have plotted these results with the Bliven *et al.* (1986) data in Figure 5. Using this data we have fitted a normalised relationship between the ratio of the measured friction velocity u_*^a and the friction velocity in the absence of low frequency waves $u_{*\mathrm{ref}}^a$ against the mean mechanically-generated wave steepness *ak*:

$$u_*^a = u_{*\mathrm{ref}}^a (1 + 9.488\, ak^{2.08}) \tag{8}$$

This relationship was used to estimate the friction velocity where directly measured data was not available.

3.2Wave Growth Rates

Measurements have been completed for four wave mechanically-generated frequencies (1.11, 1.25, 1.43 and 1.67Hz), two nominal wave steepnesses ak_0 (0.09 and 0.18) and two wind speeds (U_{cl}=7.2, and 9.3ms^{-1}). It was immediately apparent that the wind-induced wave growth rates were extremely low in comparison with the wind-induced attenuation rates in the same facility. It had been planned to gather growth data at lower frequencies and wind speeds but measurements with satisfactory confidence limits could not be made under these conditions. We selected a threshold in correlation coefficient of 0.65 and repeat measurements that satisfied this threshold for all combinations of wave frequency and wind.

The data from the present investigation has been summarised and presented with the data assembled by PB03 in Figures 6 and 7. Measurement error is indicated by bars showing the 90% confidence interval of each measurement.

The impact of the existing uncertainties in the friction velocity are immediately apparent in Figures 6 and 7. Therein the data is presented in two forms: solid squares have been used to represent the wave growth data normalised in terms of the measured friction velocities; and, solid circles show the data

normalised in terms of the stress measurements of PGP03 with no adjustment for mechanically-generated wave steepness.

In both the conventional Plant (1982) form and the drag form proposed by PB03, when normalised by the measured friction velocities, these data lie well below the measurements obtained by other investigators.

In contrast, when normalised in terms of our previously measured friction velocities the data sit naturally with the other data albeit at higher wave steepnesses than have previously been measured in detail. The only problem with this normalisation is that the data at the highest steepnesses (~0.28) in Figure 7 indicate that a higher normalised growth rate than can be supported by the total stress. However, this may merely be a result of enhanced momentum fluxes over steep waves.

MH82 measured the wind-induced growth rates of waves of the same scale exposed to wind forcing using the same techniques. In Figure 6, these measured wind-induced growth rates are superimposed as grey solid triangles. It is important to note that even using measurements of friction velocity that are comparable in magnitude with those obtained by them, the wave growth rates measured are substantially smaller than recorded by MH82. MH82 were unable to determine a systematic dependence of wave growth rate on wave steepness. Our measurements show a systematic development in normalised wave growth rate as a function of mean wave steepness as shown in Figure 7.

The results support the conclusions of PB03 that there is a systematic increase in wave growth rate when normalised by the total momentum flux. However, due to the uncertainties in the total momentum flux described above, the precise levels remain to be confirmed. If the measured total stress levels are confirmed, there is a disparity between the energy flux from the air flow observed during air-sided studies and the responding wave growth. If this is the case, it would be possible that turbulence on the water side is disrupting wave growth as contemplated by Belcher, Harris and Street (1993). If it is shown that stresses estimated from the logarithmic profiles are too high and actual values are comparable with the attenuation study, it is to be expected that the findings of PB03 will be confirmed.

For steeper waves, the proximity of the roof may be a concern. During this study, wave amplitudes up to 46mm were investigated. However, the air cavity height was approximately 450mm. For the largest waves air cavity depth above wave crests was 20% smaller than that over wave troughs. Consequently, the convergence/divergence effects in phase with the waves may have enhanced the wave growth rates. It is highly desirable to repeat these investigations with a substantially larger air cavity height.

4. AIR FLOW OBSERVATIONS

During this investigation, we endeavoured to obtained visualisation of the flow over the waves using a 0.01m thick light sheet aligned vertically down into the air cavity. Water droplets were seeded into the air flow approximately 4m upwind of the point of observation. A conventional digital camera was used to capture the streaklines produced by the water droplets within the light sheet.

A representative image captured by the camera are shown in Figure 8. Unfortunately, these do not provide conclusive evidence of air flow separation above these waves. It would appear that more sophisticated visualisation techniques similar to those used by Reul *et al.* (1999) are required to adequately capture these flow fields.

5. CONCLUSIONS AND RECOMMENDATIONS

A laboratory study of the growth of mechanically-generated waves by wind has been completed.

A number of important new observations have been obtained during this study.

The study has highlighted the importance of consideration of energy flux concomitant with momentum flux.

This study has substantially extended the findings of Bliven *et al.*, 1986 and Banner, 1990 that the total drag systematically increases with the mean wave steepness. This finding is quantitatively consistent with the Donelan (1990) observation that young wind seas exhibit higher drag than old wind seas. During this study, this effect was observed over a wider range of wave scales. However, the precise relationship between total drag and wave steepness remains to be determined but there appears to be little (<20%) enhancement up to ak=0.1. From ak=0.1 to ak~0.25, the drag increases by a factor between of 2 to 3.

However, the total drag values measured during this study are different from those obtained during the attenuation study (PGP, 2003). This aspect of the investigation but it will not be possible to progress this aspect further until measurements of total drag by an alternative method are implemented. A hot-wire anemometry system is now available to the study team and resolving this issue will be part of a future investigation.

A simple comparison of measured wave growth rates with the attenuation study shows that wind-induced growth is a weak process when compared with wind-induced attenuation.

It is clear from this investigation that there have been fundamental flaws in several previous studies of wave growth. First, this systematic increase in total drag with mean wave steepness has been ignored and therefore normalised values of growth for large wave steepnesses are too large (Bole, 1967, MH82). Also, there appears to be a fundamental problem with the conclusions of MH82. The measurements of this study were essentially a repeat of the MH82 study yet our observed growth rates were much smaller than they observed.

The proximity of the roof in undertaking these studies is a concern. The growth rates observed may have been enhanced slightly by convergence/divergence effects over the waves. It is highly desirable to repeat these investigations with a substantially larger air cavity height.

The results of this study support the conclusions of PB03 that there is a systematic increase in wave growth rate when normalised by the total momentum flux. However, due to the uncertainties in the total momentum flux described above, the precise levels remain to be confirmed. Two possibilities lie before us:

- If the measured total stress levels are confirmed, there is a disparity between the energy flux from the air flow observed during air-sided studies and the responding wave growth. If this is the case, it would be possible that turbulence on the water side is disrupting wave growth as contemplated by Belcher, Harris and Street (1993).
- If it is shown that stresses estimated from the logarithmic profiles are too high and actual values are comparable with the attenuation study, it is expected that the findings of PB03 will be confirmed.

Attempts to visualise the flow using simple illumination techniques and conventional digital video cameras have not been able to adequately capture the air flow over the waves so that the drag behaviour of the steeper waves can be determined. More sophisticated visualisation techniques will be required.

6. REFERENCES

Acton, F.S. (1959) *Analysis of Straight-Line Data.* Wylie.

Banner, M.L. (1990) The influence of wave breaking on the surface pressure distribution in wind-wave interactions. *J. Fluid. Mech.* **211**, pp 463-495

Belcher, s.E., Harris, J

Benjamin, B. and Feir, (1967)

Bliven, L.F., Hwang, N.E. and Long, S.R. (1986) Experimental study of the influence of wind on Benjamin-Feir sideband instability. *J. Fluid Mech.* **162**, 237-260

Bole, J.B. (1967) *Response of gravity water waves to wind excitation.* Ph.D. thesis. Dept. of Civil Engineering. Stanford University.

Jeffreys, H., (1924) On the formation of waves by wind. *Proc. Roy. Soc. London, Ser. A.*, **107**, 189-206

Jeffreys, H., (1925) On the formation of waves by wind, II. *Proc. Roy. Soc. London, Ser. A.*, **110**, 341-347

Kawamura, H

Kline,

Komen, G.J., Cavaleri, M., Donelan, M., Hasselmann, K., Hasselmann, S., and Janssen, P.A.E.M. (1994) *Dynamics and Modelling of Ocean Waves.* CUP.

Miles, J. W., 1957: "On the Generation of Surface Waves by Shear Flows", *J. Fluid Mech.*, 3, 185-204.

Mitsuyasu, H. (1966)

Mitsuyasu, H. and Honda, T. (1982) Wind-induced growth of water waves. *J. Fluid Mech.* (1982), **123**, 425-442Peirson, W.L., Garcia, A.W. and Pells, S.E. (2003) Water-Wave Attenuation Due To Opposing Wind. *J. Fluid Mech.* **487**, 345-365.

Peirson, W.L. and Belcher, S.E. (2003) Wave Field Development During Intense Storms. *Proceedings of the Australasian Coastal and Ports Conference. Auckland, New Zealand. September. IEAust*

Plant, W.J. (1982) A Relationship between Wind Stress and Wave Slope. *J. Geophys. Res.* **87**, No. C3, 1961-1967, March 20

Van Dorn, W.G. (1966) Boundary dissipation of oscillatory waves. *J. Fluid Mech.*, **24**, 769-779

Wright, C.W., E.J. Walsh, D. Vandemark, W.B. Krabill, A.W. Garcia, S.H. Houston, M.D. Powell, P.G. Black, and F.D. Marks (2001) Hurricane directional wave spectrum spatial variation in the open ocean, *J. Phys. Ocean.*, **31**, 2472-2488

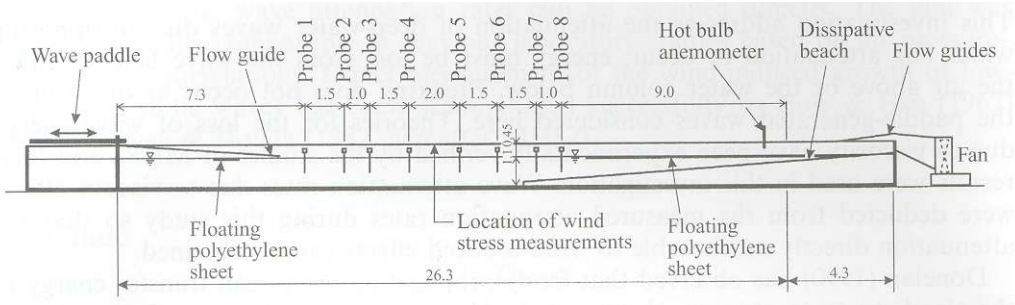

WRL Report No. 219	TANK LAYOUT	Figure 1

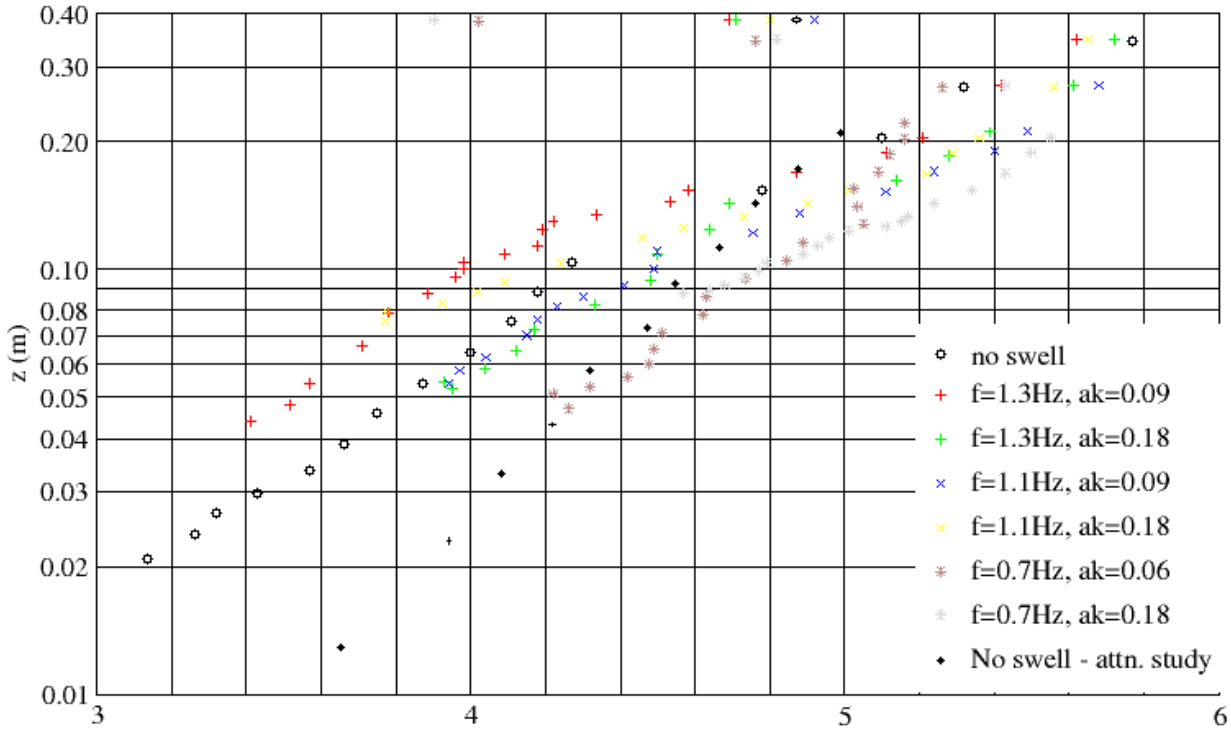

WRL Report No. 219	Air velocity profiles measured during this investigation at a wind speed of 4.8 ms^{-1} in comparison with the corresponding profile obtained during the attenuation study.	Figure 2

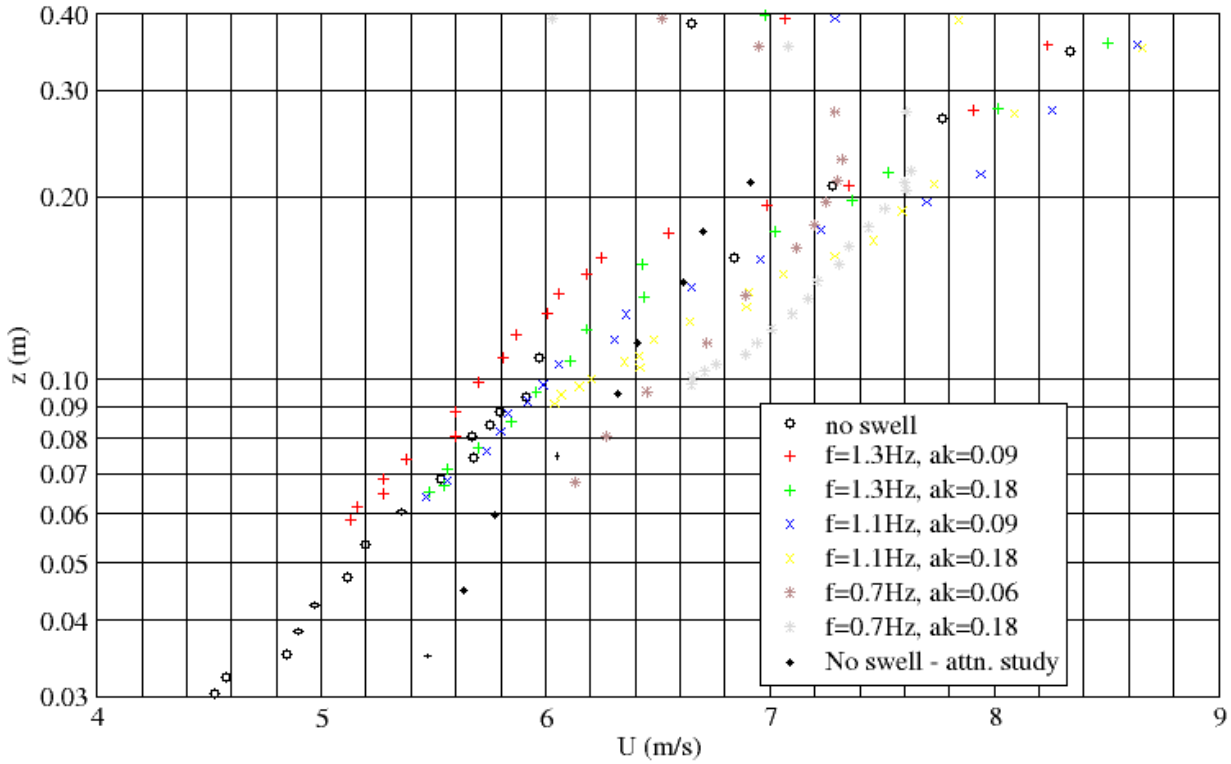

WRL Report No. 219	Air velocity profiles measured during this investigation at a wind speed of 7.2 ms^{-1} in comparison with the corresponding profile obtained during the attenuation study.	Figure 3

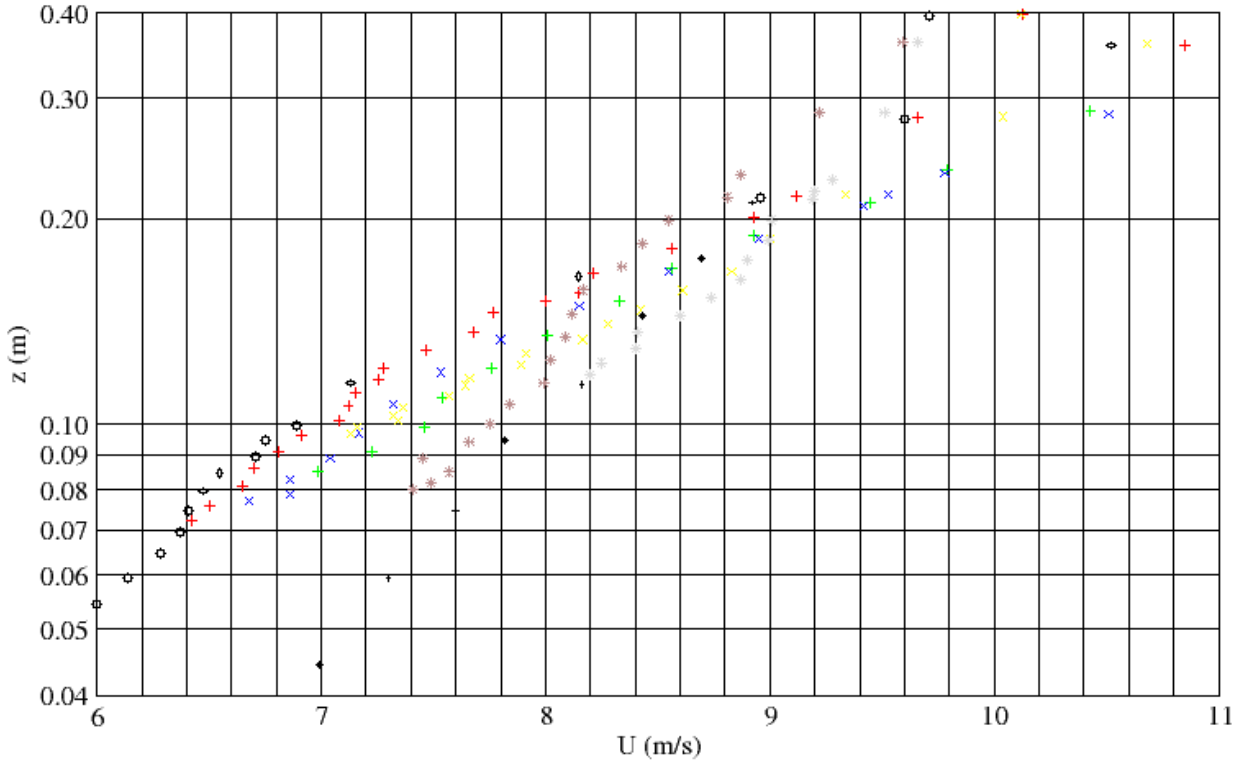

WRL Report No. 219	Air velocity profiles measured during this investigation at a wind speed of 9.3 ms^{-1} in comparison with the corresponding profile obtained during the attenuation study.	Figure 4

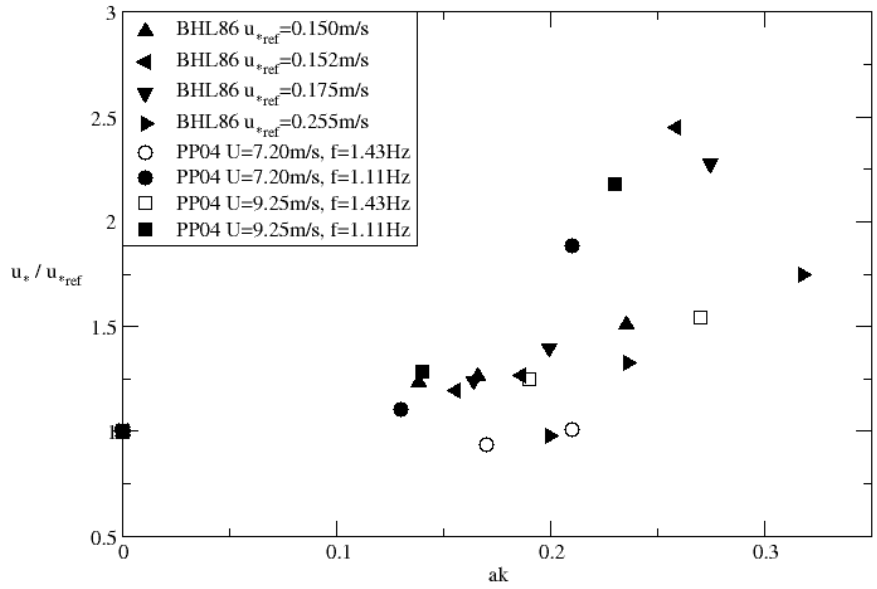

Note:
1. BLS86 denotes data extracted from the study by Bliven *et al.*(1986).
2. PP04 denotes data obtained during this study.

WRL Report No. 219	Measured friction velocity as ratio of that measured in the absence of mechanically-generated waves presented as a function of mean mechanical wave steepness.	Figure 5

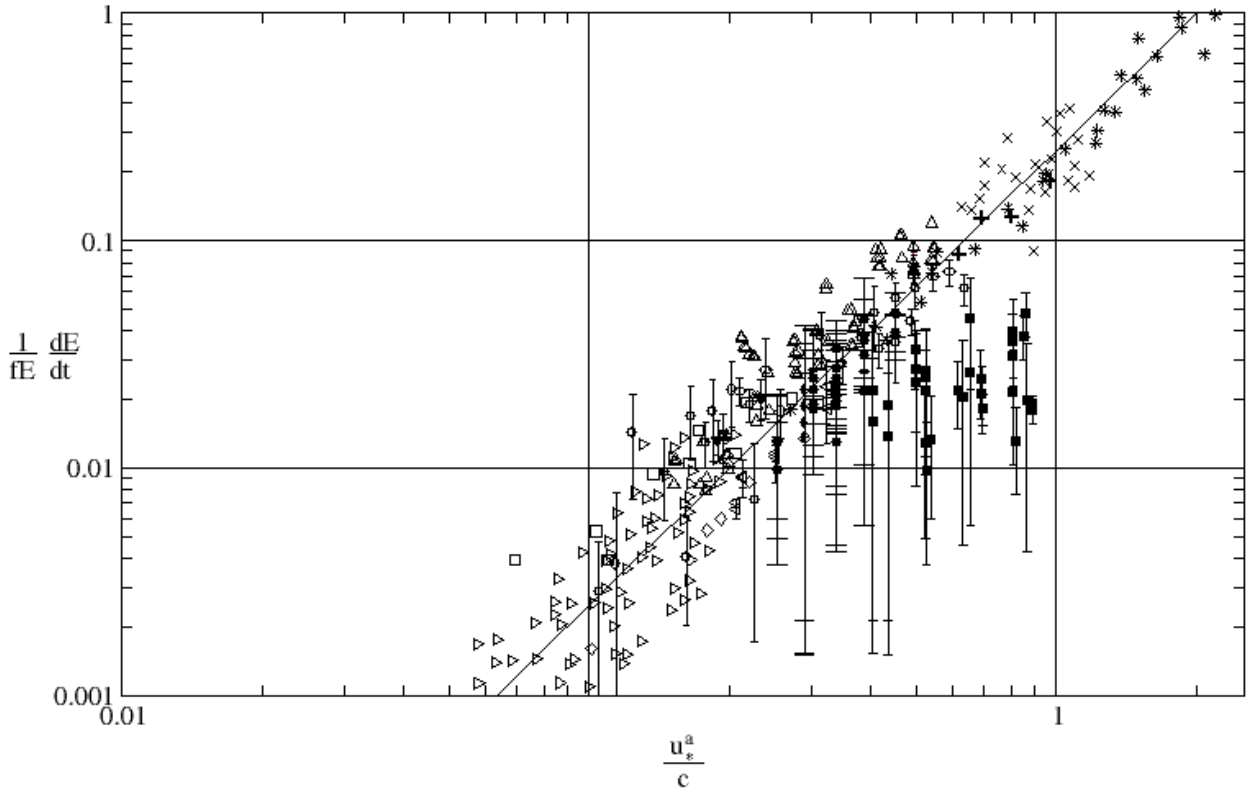

Symbols indicate as follows: asterices, Larson and Wright, 1974; x, data from Wu, Hsu and Street (1977); diamonds, Shemdin and Hsu, 1971; triangles to right, Snyder et al., 1981; solid circles, Bole, 1967; solid squares, Wilson et al., 1971; + Banner, 1990; triangles to left, Bliven et al., 1986; upright triangles, Mitsuyasu and Honda, 1982; downward pointing triangles, Mastenbroek et al., 1996.

Solid circles indicate the growth rates obtained from this investigation using the stress measurements of PGP03 at comparable wind speeds with no adjustment for the mechanically-generated wave steepness. The solid squares indicate the growth rates obtained from this investigation using the stress measurements of this study.

WRL Report No. 219	Wave growth data assembled by Plant (1982) with data obtained from other investigations as shown. Error bars indicating 90% confidence limits have been specified where possible.	Figure 6

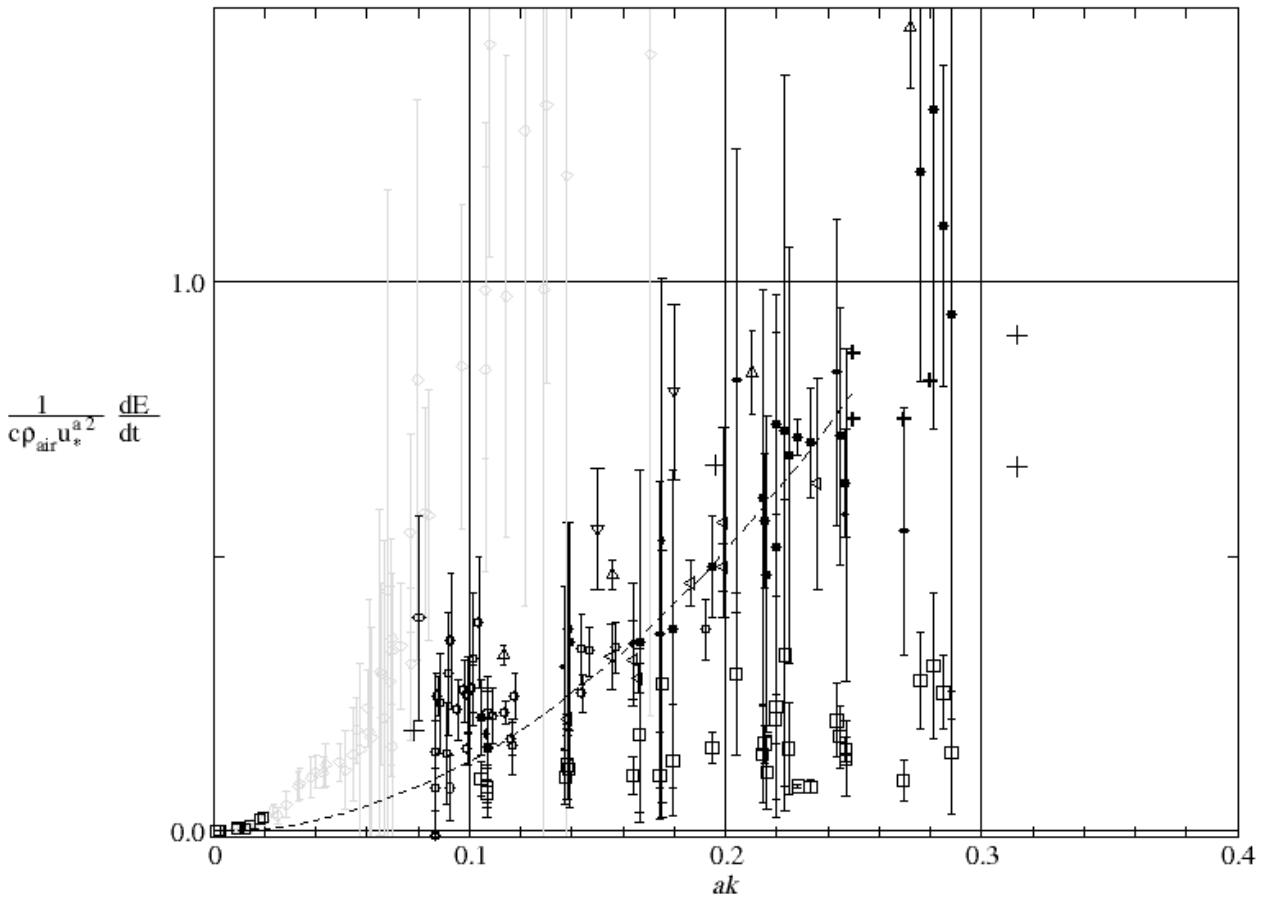

Symbols indicate as follows: hollow circles, Bole, 1967; small hollow squares, Wilson *et al.*, 1971; + Banner, 1990; triangles to left, Bliven *et al.*, 1986; upright triangles, Mitsuyasu and Honda, 1982; downward pointing triangles, Mastenbroek *et al.*, 1996. Corresponding form drag data from BNH93 of flow over sinusoidal solid hills has been added with the ratio of form drag to total drag on the ordinate: solid diamonds: measurements by Zilker and Hanratty, 1979; small solid squares, mixing length model; dotted line, model results for second order closure. The magnitudes of non-breaking wave energy loss in the presence of an opposing wind by Peirson *et al.*, 2003 are shown as grey hollow diamonds.

Solid circles indicate the growth rates obtained from this investigation using the stress measurements of PGP03 at comparable wind speeds with no adjustment for the mechanically-generated wave steepness. The large hollow squares indicate the growth rates obtained from this investigation using the stress measurements of this study.

WRL Report No. 219	Measured wind energy input to monochromatic waves as a function of wave steepness.	Figure 7

Best visualisation result achieved with injected water droplets and conventional DV camera. Bright line is the meniscus on the near side wall and upper bright profile is the wave profile at the light sheet. Although droplets were visible to the eye higher in the cavity, they are not visible adjacent to the surface.

WRL Report No. 219	Preliminary visualisations of air flow over the waves. Upper panel shows the best result	Figure 8

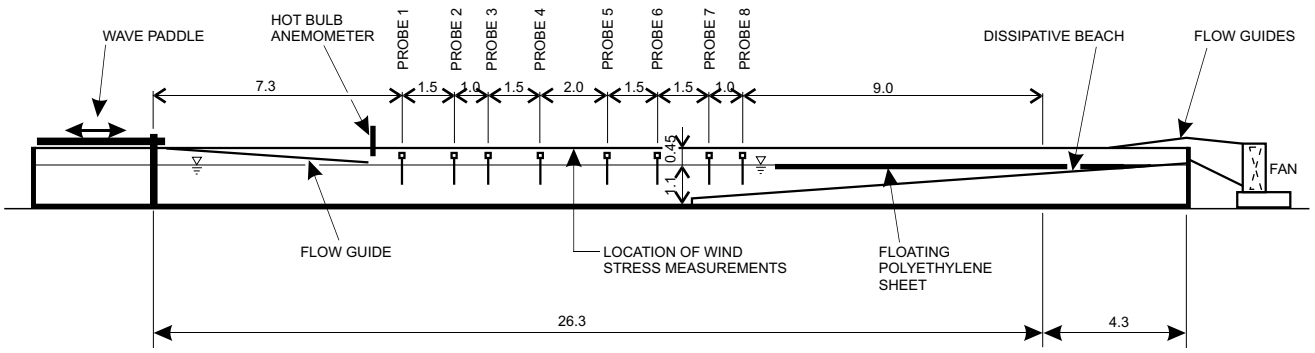

WRL Report No. 219	TANK LAYOUT	Figure 1 219-01.cdr

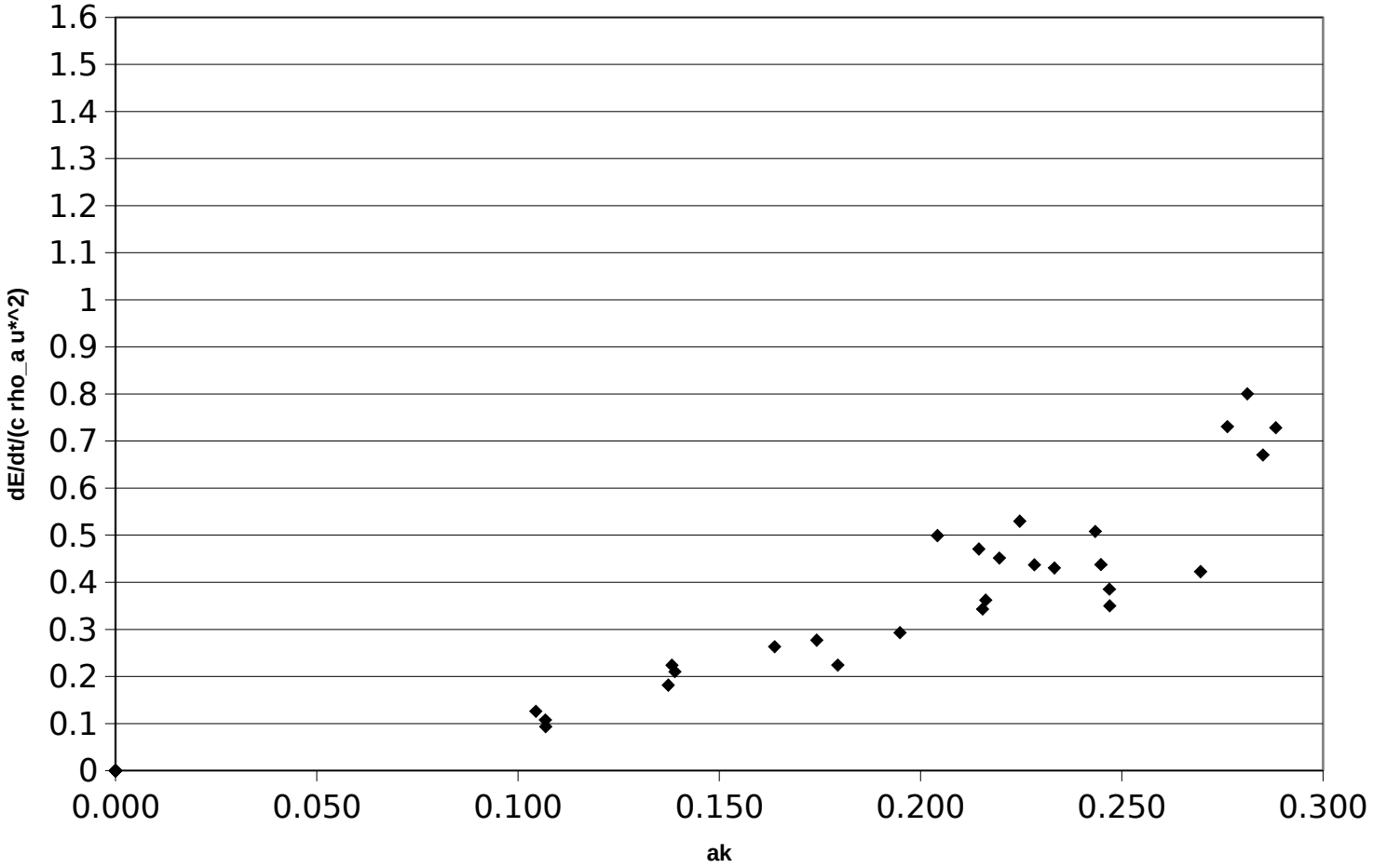
dE/dt/(c rho_a u*^2)
1.6
1.5
1.4
1.3
1.2
1.1
1
0.9
0.8
0.7
0.6
0.5
0.4
0.3
0.2
0.1
0
0.000
0.050
0.100
0.150
0.200
0.250
0.300
ak